

# Correlation of ultrasound perfusion imaging and angiogenesis of ovarian tumors

X. Liu and C. Shen\*

<sup>1</sup>Department of Ultrasound, Huangshi Maternity & Children's Health Hospital, Edong Healthcare. Huangshi, Hubei, 435000

## ABSTRACT

**Background:** The aim of this present study was to evaluate the relationship between perfusion characteristics of ovarian tumors and tumor angiogenesis using contrast-enhanced ultrasound imaging. **Materials and Methods:** Dose 116 patients with ovarian tumors were preoperatively subjected to contrast-enhanced perfusion imaging. Immunohistochemistry was performed to detect the expression of vascular endothelial growth factor (VEGF) and CD34 in ovarian tumors. The correlation between the VEGF positive index, microvessel density (MVD) of ovarian tumors and ultrasound perfusion parameters was investigated. We also established a nude mouse ovarian cancer SKOV3 xenograft model; the expression of VEGF and MVD in the transplanted tumor was observed, and their correlation with the ultrasound perfusion parameters was studied. **Results:** The MVD and VEGF positive indexes of ovarian tumors were positively correlated with the peak intensity (PI), area under the curve (AUC) and time from peak to one half (TTH) of the ultrasound perfusion parameters. The correlation coefficients between MVD and the PI, AUC and TTH were 0.69, 0.71 and 0.59, respectively, while the correlation coefficients between the VEGF positive index and the PI, AUC and TTH were 0.71, 0.65 and 0.68, respectively. Moreover, there were significant differences in the PI, AUC and TTH between the high-MVD and low-MVD groups ( $P < 0.05$ ). Furthermore, the same trend was found in the xenograft model. **Conclusion:** the ultrasound perfusion parameters PI, AUC and TTH of ovarian tumors were positively correlated with the tumor MVD and VEGF positive index, which reflects the angiogenesis status of ovarian tumors and provides important information for the diagnosis and treatment of ovarian tumors.

**Keywords:** Ovarian tumors, Ultrasound perfusion imaging, Angiogenesis, Perfusion parameters.

## ► Original article

### \*Corresponding authors:

Cui Shen, MD,

### E-mail:

[shencui198403@163.com](mailto:shencui198403@163.com)

Revised: January 2019

Accepted: March 2019

Int. J. Radiat. Res., October 2019;  
17(4): 559-567

DOI: 10.18869/acadpub.ijrr.17.3.559

## INTRODUCTION

Tumor angiogenesis refers to the process initiating from the pre-microvascular stage to the growth of capillaries into new blood vessels<sup>(1)</sup>. Studies on angiogenesis of ovarian cancer have demonstrated a significant correlation of the angiogenesis with the prognosis in ovarian cancer. Ovarian tumor tissue exhibits an abnormally rich vascular network and new angiogenesis, which provide a material basis for tumor tissue growth and an important pathway

for tumor metastasis. Microvessel density (MVD) is the gold standard for evaluating vascular conditions and is often used to evaluate and quantify vascular conditions in biopsy tissues<sup>(2)</sup>. MVD is a non-imaging method with certain limitations. First, it is invasive, and it is necessary to obtain a disease tissue to measure MVD. Second, the distribution of blood vessels in a tumor is not uniform; MVD cannot measure the whole tumor and only reflects the blood vessels in the local tissue to be measured. Therefore, MVD does not necessarily represent the vascular

condition of the whole tumor.

Developing an imaging technology that can non-invasively evaluate the microcirculation state of the whole tumor is a research hotspot. Contrast-enhanced perfusion imaging is a non-invasive functional imaging method <sup>(3)</sup>. Quantitative analysis of the blood flow in the region of interest can be performed by injecting a microbubble contrast agent to quantitatively analyze the blood flow information in the region of interest. Zhou et al found that the targeted ultrasound agent can bind with angiogenesis endothelium in ovarian transplantation tumor of nude mice and achieved targeted ultrasound molecular imaging, which provide a new method on ovarian cancer angiogenesis evaluation <sup>(4)</sup>. So far, there have been only few reports on CEUS characteristics and their relationship with MVD in benign and malignant ovarian lesions. The purpose of this present study was to evaluate the relationship between the perfusion characteristics of ovarian tumors and tumor angiogenesis using contrast-enhanced ultrasound imaging.

## **MATERIALS AND METHODS**

### ***Patients***

All patients with ovarian tumors who were clinically diagnosed and confirmed via postoperative pathological examination from January 2016 to December 2018 were enrolled. All patients underwent ultrasound contrast perfusion imaging within 3 days before surgery. Patients were included and excluded according to the following criteria. The inclusion criteria were cases diagnosed as ovarian tumors via a clinical diagnosis and postoperative pathological examination. The exclusion criteria were obvious cardiopulmonary abnormalities; a history of obvious allergies; body mass index exceeding 25 kg/m<sup>2</sup>; postoperative pathological findings indicating non-ovarian tumors; poor perfusion image quality during the scanning process due to patient movement or respiratory motility and the inability to perform quantitative analysis; and the inability to immunohistochemi-

cally stain the pathological specimen. This work was approved by the Ethics Committee of Huangshi Maternity & Children's Health Hospital, and informed consent was obtained from all patients. Finally, 116 patients were enrolled. Out of a total of 116 ovarian tumors, 40 were benign ovarian tumors and 76 were malignant ovarian tumors.

### ***Ovarian cancer xenograft model***

The ovarian cancer xenograft model was established as previously described <sup>[5]</sup>. Briefly, human ovarian cancer cells SKOV3 (Cell Bank of the Chinese Academy of Sciences) were subcutaneously injected for 28 d into the back of 30 Balb/c female nude mice (Institute of Laboratory Animals, Chinese Academy of Medical Sciences) that were 7-8 weeks old and that had body weights of 18-20 g. The nude mice were sacrificed according to the ethical requirements for experimental animals.

### ***Equipment***

The study was performed using a GE-Voluson E10 ultrasound system (General Electric Company, Fairfield, Connecticut, USA) with a transducer frequency range of 5.0 to 9.0 MHz. Contrast-specific imaging (CSI) mode was used for contrast-enhanced ultrasound at a low mechanical index (<0.2), enabling efficient tissue elimination to produce almost pure microbubble images and avoid microbubbles in microcirculation damage.

### ***Routine Ultrasound Examination***

Conventional ultrasonography was used to obtain a comprehensive two-dimensional gray-scale image of the pelvic internal organs (such as the uterus and adnexa); the position, size, shape, boundary, ultrasonic properties, envelope and internal echo of the tumor were observed for the detected lesions. Color Doppler ultrasound was used to observe the blood flow.

### ***Contrast-enhanced perfusion imaging***

The contrast agent (SonoVue, Bracco, Italy) consisted of sulfur hexafluoride (SF<sub>6</sub>) surrounded by a phospholipid. After 2.4 ml (0.3

ml for mouse) of the microbubble suspension was injected into the vein, a single injection of 5 mL of normal saline was administered. After using conventional ultrasound to observe and determine the lesion, the method was switched to the ultrasound contrast mode, the cut surface was fixed to the largest section of the tumor to display part of the uterus, and the method was switched to the double contrast mode. The contrast image was dynamically observed continuously.

### **Image Analysis**

The regions of interest (ROI) of the lesions were selected first, and the ovarian cystic mass was selected from the thickest part of the cyst wall. The ROI was selected as the ovarian solid mass in the largest longitudinal section of the mass; the free shape delineation method or fixed 5 mm box delineation method was used to avoid the capsule and the hyperechoic area of the mass, which may be a large vessel or a non-blood perfusion zone. The ROI position was corrected frame by frame, and frames with excessively displaced organs were removed to ensure that the ROI was located within the tumor throughout image analysis. The time-intensity curve (TIC) was obtained; the gamma fitting function suitable for the group injection method was selected to perform gamma curve fitting on the TIC; and the contrast perfusion parameters of the lesion site were obtained, including the rise time (RT), peak intensity (PI), area under the curve (AUC), time from peak to one half (TTH), and time to peak (TT).

### **Immunohistochemistry**

The specimens were placed according to their anatomical position, the longitudinal section of the largest lesion was vertically cut, and the tissue in the deepest infiltrating area of the surrounding tissue was removed. After obtaining the specimen, it was fixed in neutral formalin for 4-6 hours and embedded in paraffin. The paraffin block was sliced into 4  $\mu$ m slices on a common slide, and HE staining was performed to determine the histological type and tissue structure. Immunohistochemical

staining was performed using the streptavidin-peroxidase method. The primary antibody CD34 (sc-74499, 1:100, Santa Cruz Biotechnology, Inc.) is a mouse monoclonal antibody raised against amino acids 151-290 of CD34 of human or mouse origin, while the VEGF antibody (sc-7269, 1:150, Santa Cruz Biotechnology, Inc.) is a mouse monoclonal antibody raised against amino acids 1-140 of VEGF of human or mouse origin.

### **Determination of results**

VEGF evaluation criterion: Brown-yellow particles appear in the cytoplasm of ovarian tumor cells as a criterion for VEGF-positive cells. VEGF grading of ovarian tumors was performed according to the method of Siddiqui *et al.* <sup>(6)</sup>: the staining intensity was divided into 4 degrees; degree 0 was no staining in the cytoplasm of ovarian tumor cells, degree 1 was cytoplasmic staining of ovarian tumor cells, degree 2 was medium cytoplasmic staining of ovarian tumor cells, and degree 3 was stronger in cytoplasmic staining of ovarian tumor cells. According to the percentage of stained ovarian tumor cells in all observed cells, they were divided into 4 grades: grade 0 showed no stained ovarian tumor cells; grade 1 indicated stained ovarian tumor cells  $\leq 25\%$ ; grade 2 indicated stained ovarian tumor cells  $>25\%$  and  $\leq 50\%$ ; and grade 3 indicated stained ovarian tumor cells  $>50\%$ . The scores of the staining intensity and percentage were added to obtain a VEGF positive index.

MVD evaluation criterion: Cells with brown-yellow particles after CD34 staining in the cytoplasm were identified as vascular endothelial cells. MVD counts of ovarian tumors were performed according to the method of Huang *et al.* <sup>(7)</sup>: if the surrounding adjacent tissue could be distinguished from the brown-colored vascular endothelial cells, it was judged to be a microvessel. Large blood vessels containing smooth muscle wall or vascular lumen greater than approximately 8 red blood cells were not counted in the MVD count of ovarian tumors; the average of 5 visual fields was taken as the representative value of MVD of ovarian tumors.

### Statistical analysis

Statistical analysis was performed using SPSS version 19.0 (Chicago, IL, USA). Data are expressed as the mean  $\pm$  SD of at least three independent experiments. Spearman correlation analysis was used to analyze the relationship between the VEGF positive index and MVD in ovarian tumors and the correlation between the perfusion parameters of ovarian tumors, VEGF positive index and MVD. The VEGF positive index and MVD of ovarian tumors in different clinical pathological conditions were analyzed using one-way analysis of variance or Student's *t*-test. All differences were considered statistically significant at the level of  $P < 0.05$ .

## RESULTS

### VEGF and MVD immunohistochemistry results

As shown in figure 1 (A, B), ovarian tumors were stained positive for VEGF and CD34, and the positive rate was 100%. The MVD of 40 cases of ovarian benign tumors was  $(32.19 \pm 7.25)/\text{HP}$ , and the MVD of 76 cases of ovarian cancer was  $(57.27 \pm 9.28)/\text{HP}$ . The VEGF positive index of 40 cases of benign ovarian tumors was  $3.86 \pm 0.45$ , and that of 76 cases of malignant ovarian tumor was  $6.87 \pm 1.12$ ; the difference was statistically significant ( $P < 0.01$ ). Furthermore, correlation analysis found that the VEGF positive index was positively correlated with MVD (table 1) ( $r=0.52$ ,  $P < 0.05$ ;  $r=0.65$ ,  $P < 0.05$ ).

### Relationship between the VEGF positive index and MVD and the clinical characteristics of human ovarian cancer

As shown in table 2, among the 76 cases of malignant tumors, 10 cases were stage I, 16 cases were stage II, 20 cases were stage III, and 30 cases were stage IV; 50 cases exhibited poor differentiation, and 26 cases exhibited high differentiation; 40 cases exhibited lymph node metastasis, and 36 cases exhibited no lymph node metastasis; and 30 cases were metastatic malignant tumors, and 46 cases were primary malignant tumors. The VEGF positive index and MVD of ovarian cancer were compared with

respect to the clinical stage, differentiation degree, lymph node metastasis, and primary or metastasized tumor. The results showed no significant difference ( $P > 0.05$ ).

### Correlation between MVD and the VEGF positive index and ultrasound perfusion parameters of ovarian cancers

Ultrasound contrast perfusion images of ovarian tumors are shown in figure 1(C, D). The correlation between MVD and the VEGF positive index and perfusion parameters in 116 ovarian tumors is shown in table 3. The perfusion parameter RT was  $(15.38 \pm 7.41)$  s, PI was  $(18.23 \pm 5.69)$  dB, AUC was  $(1125.54 \pm 452.98)$  dB·s, TTH was  $(58.23 \pm 22.46)$  s and TTP was  $(38.19 \pm 15.58)$  s. The Spearman correlation coefficients of MVD and the PI, AUC and TTH were 0.69, 0.71 and 0.59, respectively ( $P < 0.05$ ), while the Spearman correlation coefficients of the VEGF positive index and the PI, AUC and TTH were 0.71, 0.65 and 0.68, respectively ( $P < 0.05$ ).

Moreover, the relationship between MVD and the VEGF positive index and perfusion parameters in 30 cases of transplanted tumors is shown in table 4. The perfusion parameter RT was  $(8.52 \pm 6.37)$  s, PI was  $(31.79 \pm 8.52)$  dB, AUC was  $(305.73 \pm 89.75)$  dB·s, TTH was  $(60.17 \pm 35.12)$  s and TTP was  $(35.48 \pm 17.51)$  s. The Spearman correlation coefficients of MVD and the PI, AUC and TTH were 0.51, 0.65 and 0.58, respectively ( $P < 0.05$ ), while the Spearman correlation coefficients of the VEGF positive index and the PI, AUC and TTH were 0.61, 0.60 and 0.55, respectively ( $P < 0.05$ ).

### Comparison of the ultrasound perfusion parameters between high and low MVD

In human ovarian cancers, 38/HP was used as the critical value according to the ROC curve. Cases with  $\text{MVD} \geq 38/\text{HP}$  were considered to be the high-MVD group ( $n=46$ ), and cases with  $\text{MVD} < 38/\text{HP}$  were considered to be the low-MVD group ( $n=30$ ). The perfusion parameters of the two groups are compared in table 5. The difference among the groups of the PI, AUC and TTH was statistically significant ( $P < 0.01$ ). The PI, AUC and TTH for the high-MVD group were significantly higher than those for the low-MVD

group.

In transplanted tumors of nude mice, 35/HP was used as the critical value according to the ROC curve, and cases with MVD  $\geq 35$ /HP were considered to be the high-MVD group (n=24) and cases with MVD  $< 35$ /HP were considered to be the low-MVD group (n=6). The perfusion

parameters of the two groups are compared in table 6. The difference among the groups of the PI, AUC and TTH was statistically significant ( $P < 0.01$ ). The PI, AUC and TTH for the high-MVD group were significantly higher than those for the low-MVD group.

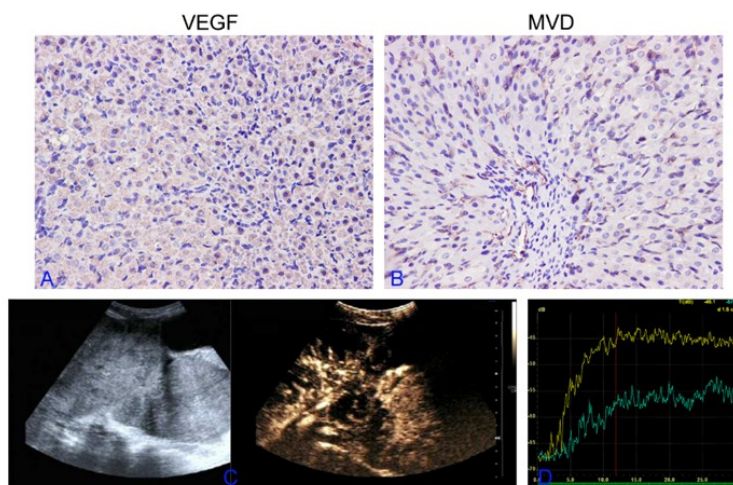


**Figure 1.** Immunohistochemistry stains and ultrasound perfusion imaging of ovarian tumors. A: Immunohistochemistry stains of VEGF, magnification  $\times 400$ ; B: immunohistochemistry stains of CD34, which represents the distribution of microvessels, original magnification  $\times 400$ ; C: ultrasound perfusion imaging of ovarian tumors; D: the time-intensity curve (TIC) of the ultrasound perfusion.

**Figure 1.** Modified Ondo Google Satellite Map Showing Zones of Sample Collection. Map data ©2017 Google (14).

	benign ovary tumor (n=40)	malignant ovary tumor (n=76)	P
MVD(/HP)	32.19 $\pm$ 7.25/HP	57.27 $\pm$ 9.28/HP	0.000
VEGF index	3.86 $\pm$ 0.45	6.87 $\pm$ 1.12	0.000
r	0.52	0.65	
P	0.010	0.008	

**Table 2.** Relationship between VEGF positive index and MVD with clinicopathological features of malignant ovarian cancer.

Clinical characteristics	classification	case	MVD(/HP)	P	VEGF index	P
clinical stage	phase I	10	58.3 $\pm$ 8.5	0.12	6.9 $\pm$ 2.5	0.15
	phase II	16	60.7 $\pm$ 12.1		5.8 $\pm$ 1.9	
	phase III	20	53.5 $\pm$ 5.7		6.5 $\pm$ 3.4	
	phase IV	30	55.7 $\pm$ 9.6		5.3 $\pm$ 1.2	
differentiation	poorly	50	60.5 $\pm$ 7.8	0.09	5.2 $\pm$ 1.5	0.08
	well	26	57.9 $\pm$ 5.4		6.1 $\pm$ 2.3	
lymph node metastasis	yes	40	58.3 $\pm$ 8.2	0.13	5.5 $\pm$ 2.1	0.34
	no	36	55.9 $\pm$ 4.8		5.9 $\pm$ 1.3	
primary or metastatic	metastatic	30	61.1 $\pm$ 11.1	0.16	7.2 $\pm$ 2.2	0.16
	primary	46	55.3 $\pm$ 6.5		6.5 $\pm$ 1.9	

Table 3. The spearman correlation between perfusion parameters and MVD and VEGF positive index of ovarian cancers.

Perfusion parameter		MVD		VEGF	
		r	P	r	P
RT(s)	15.38±7.41	0.19	0.85	0.26	0.23
PI(dB)	18.23±5.69	0.69	0.02	0.71	0.00
AUC(dB.s)	1125.54±452.98	0.71	0.01	0.65	0.03
TTH(s)	58.23 ±22.46	0.59	0.00	0.68	0.01
TTP(s)	38.19±15.58	-0.15	0.53	-0.21	0.32

RT: Rise time; PI: Peak intensity; AUC: Area under the curve; TTH: Time from peak to one half; TTP: Time to peak; MVD: Microvessel density; VEGF: Vascular epithelial growth factors.

Table 4. The spearman correlation between perfusion parameters and MVD and VEGF positive index of transplanted tumors.

Perfusion parameter		MVD		VEGF	
		r	P	r	P
RT(s)	8.52±6.37	0.18	0.32	0.09	0.41
PI(dB)	31.79±8.52	0.51	0.03	0.61	0.02
AUC(dB.s)	305.73±89.75	0.65	0.00	0.60	0.04
TTH(s)	60.17 ±35.12	0.58	0.01	0.55	0.03
TTP(s)	35.48±17.51	-0.11	0.29	-0.23	0.71

RT: Rise time; PI: Peak intensity; AUC: Area under the curve; TTH: Time from peak to one half; TTP: Time to peak; MVD: Microvessel density; VEGF: Vascular epithelial growth factors.

Table 5. Comparison of ultrasound perfusion parameters between high MVD group and low MVD group of ovarian tumors.

Perfusion parameter	Low MVD group (n=30)	High MVD group(n=46)	P
RT(s)	16.12±9.32	14.31±4.12	0.323
PI(dB)	16.32±4.43	19.89±4.52	0.001
AUC(dB.s)	890.31±359.01	1300.35±401.57	0.000
TTH(s)	50.15±18.23	64.12±12.45	0.000
TTP(s)	38.23±5.32	36.72±2.11	0.147

RT: Rise time; PI: Peak intensity; AUC: Area under the curve; TTH: Time from peak to one half; TTP: Time to peak; MVD: Microvessel density.

Table 6. Comparison of ultrasound perfusion parameters between high MVD group and low MVD group of transplanted tumors.

Perfusion parameter	Low MVD group (n=6)	High MVD group(n=24)	P
RT(s)	7.69±2.32	8.31±4.12	0.632
PI(dB)	24.25±4.57	32.99±2.19	0.005
AUC(dB.s)	250.56±58.01	356.91±68.29	0.004
TTH(s)	50.91±12.68	65.52±3.23	0.037
TTP(s)	42.12±8.78	38.25±3.98	0.336

RT: Rise time; PI: Peak intensity; AUC: Area under the curve; TTH: Time from peak to one half; TTP: Time to peak; MVD: Microvessel density.

## DISCUSSION

### **Angiogenesis of ovarian tumors**

In 1971, Folkman *et al.* <sup>(8)</sup> first proposed a theory that tumor growth and metastasis depend on tumor angiogenesis. Studies have shown that when inhibiting tumor angiogenesis, tumor tissue growth often cannot exceed 2 to 3 mm<sup>3</sup> and will be in a sleep state <sup>(9)</sup>. Depending on the presence or absence of blood vessels, the growth of the tumor can be divided into two distinct phases: a slow-growing avascular phase and a rapidly growing proliferative vascular phase. Compared with normal blood vessels, neovascular tumors have the following characteristics in terms of morphology and function: increased number of blood vessels; increased permeability of the wall; increased arteriovenous shunt; slender, fragile and tortuous neovascularization; lack of smooth muscle in the wall; presence of vascular end veins; discontinuous and regurgitating blood flow in the blood vessels; tumor interstitial tissue with increased pressure; and increased hematocrit <sup>(10)</sup>. The characteristics of the above tumor blood vessels cause changes in tumor blood perfusion parameters, which is also the pathological basis of ultrasound perfusion imaging.

### **Relationship between MVD and VEGF in ovarian tumors**

Tumor angiogenesis can be understood by measuring the expression of MVD and VEGF in tissues. MVD is considered to be the gold standard for evaluating tissue vascular conditions and is often used to evaluate and quantify vascular conditions in biopsy tissues. In this study, the MVD of benign ovarian tumors was lower than that of ovarian cancer, and the difference was statistically significant, indicating that MVD is related to the malignant condition of the tumor. These results are similar to those obtained from studies conducted at home and abroad <sup>(11)</sup>. However, the results of the present study suggest that MVD is not associated with the stage, differentiation, presence of primary or secondary tumors of the ovarian cancer and whether the tumor has lymph node metastasis.

Tumor angiogenesis is regulated by both angiogenesis inhibitors and stimulators. VEGF is the most important stimulating factor to promote tumor angiogenesis <sup>(12)</sup>. VEGF is a glycoprotein whose biological function is mainly to promote the division and proliferation of endothelial cells in blood vessels, thereby promoting the neovascularization of tissues, inhibiting the apoptosis process of vascular endothelial cells, and increasing the permeability of microvessel in tissues <sup>(13)</sup>. Studies have shown that VEGF has a very close relationship with the formation of tumor angiogenesis <sup>(14)</sup>. In the present study, the positive expression rate of VEGF in 116 cases of ovarian tumors was as high as 100% and the VEGF positive index of benign ovarian tumors was lower than that of ovarian cancer. The difference was statistically significant, consistent with results that have been reported in the literature <sup>(15-17)</sup>. However, this study suggests that the VEGF positive index is not associated with the stage, differentiation, tumor lymph-node metastasis status and presence of a primary tumor in ovarian cancer. Patients with positive VEGF expression often exhibit higher MVD <sup>(18-19)</sup>. In the present study, we also investigated the correlation between the VEGF positive index and MVD in ovarian tumors, and correlation analysis indicated that the VEGF positive index was positively correlated with MVD in both benign and malignant ovarian tumors ( $r=0.52$ ,  $P<0.05$ ;  $r=0.65$ ,  $P<0.05$ ).

### **Relationship between ultrasound perfusion parameters and MVD and VEGF**

Many previous studies have shown that tumor angiogenesis is associated with ultrasound perfusion parameters. Ultrasound perfusion imaging is a non-invasive and quantitative analysis technique for determining the vascular conditions in tumors. Ultrasound perfusion imaging is safe, convenient, non-invasive, reproducible and easy to use repeatedly. This study analyzed the correlation between MVD and the VEGF positive index and ovarian tumor ultrasound perfusion parameters. The results showed that the MVD and VEGF positive index of ovarian tumor were positively

correlated with the perfusion parameters PI, AUC and TTH, which exhibited no correlation with other perfusion parameters. Comparing the high-MVD with the low-MVD ultrasound perfusion parameters, the difference in the PI, AUC and TTH between the two groups was statistically significant ( $P < 0.05$ ). Of note, we also added the xenograft model experiment, in the transplanted tumors of nude mice, we observed the same trend as human ovary tumors. In the previous study, Willmann *et al.* also found that contrast-enhanced ultrasound directed at VEGFR2 improves *in-vivo* visualization of tumor angiogenesis in a human ovarian cancer xenograft tumor model in mice <sup>(20)</sup>.

The PI refers to the maximum value of the time-intensity curve, which characterizes the maximum concentration of contrast agent or the blood volume. The AUC refers to the area under the entire time-intensity curve, which characterizes blood volume, and the AUC is proportional to the regional blood volume. The TTH refers to the time when the curve intensity decreases from the peak to half of the peak, characterizing the flow rate of blood flushing, which is the contrast-agent removal time; the contrast agent content is related to the amount of perfusion of the tissue <sup>(21-23)</sup>. Tumor neovascularization is characterized by the pathology of the changes in the ultrasound perfusion parameters of tumor blood flow. In this study, 3 perfusion parameters (PI, AUC and TTH) that were associated with the tissue blood volume were positively correlated with MVD and the VEGF positive index, demonstrating that the tumor blood volume is closely related to the tumor microvascular status and that tumor-induced microvascular changes often manifest as an increase in tumor perfusion <sup>(24)</sup>. Wang's study also found that the PI and AUC of the ovarian masses in the contrast transvaginal sonography show significant correlation with the angiogenesis and may help in assessing tumor vascularity in ovarian masses <sup>(25)</sup>. Therefore, we believe that the PI, AUC and TTH are important indicators of the expression of MVD and VEGF.

In conclusion, this study explored the correlation between contrast-enhanced

perfusion imaging and angiogenesis in human ovarian tumors and transplanted ovarian tumors and found that the PI, AUC and TTH, as perfusion parameters, were associated with ovarian tumor MVD and VEGF. The PI, AUC and TTH can reflect the angiogenesis status of ovarian tumors and have the potential to serve as prognostic factors.

### Authors' contributions

Xin Liu performed the experiments and wrote the paper, Cui Shen designed the study and reviewed the manuscript. All authors discussed the results and approved the final manuscript.

**Conflicts of interest:** Declared none.

## REFERENCES

1. Mentzer SJ and Konerding MA (2014) Intussusceptive angiogenesis: expansion and remodeling of microvascular networks. *Angiogenesis*, **17**: 499-509.
2. Lafora JBM and Aranda FI (2015) Angiogenic Index: A new method for assessing micro vascularity in breast carcinoma with possible prognostic implications. *Breast J*, **6**: 103-107.
3. Harvey CJ, Pilcher JM, Eckersley RJ, *et al.* (2002) Advances in ultrasound. *Clin Radiol*, **57**: 157-177.
4. Zhou Q, Liu H, Xiang H, *et al.* (2017) Assessment of targeting ultrasound contrast agent on vasculogenic mimicry in ovarian cancer. *Chinese J Ultrasound Med*, **33**: 349-352.
5. Hermanson DL, Bendzick L, Kaufman DS (2016) Mouse xenograft model for intraperitoneal administration of NK cell immunotherapy for ovarian cancer. *Methods Mol Biol*, **1441**: 277-84.
6. Siddiqui GK, Elmasry K, Wong AC, *et al.* (2010) Prognostic significance of intratumoral vascular endothelial growth factor as a marker of tumour angiogenesis in epithelial ovarian cancer. *Eur J Gynaecol Oncol*, **31**: 156-159.
7. Huang X, Chen L, Fu G, *et al.* (2012) Decreased expression of pigment epithelium-derived factor and increased microvascular density in ovarian endometriotic lesions in women with endometriosis. *Eur J Obstet Gyn RB*, **165**: 104-109.
8. Folkman J (1971) Tumour angiogenesis: Therapeutic implication. *N Eng J Med*, **285**: 1182-1186.
9. Ebos JM, Lee CR, Cruzmunoz W, *et al.* (2009) Accelerated metastasis after short-term treatment with a potent inhibitor of tumor angiogenesis. *Cancer Cell*, **15**: 232-239.

10. Satoh A, Shuto K, Okazumi S, *et al.* (2010) Role of perfusion CT in assessing tumor blood flow and malignancy level of gastric cancer. *Digest Surg*, **27**: 253-260.
11. Xie L, Shen LD, Qing C, *et al.* (2012) Correlational study of vascular endothelial growth factor expression and microvessel density in primary malignant gastric lymphoma. *Med Oncol*, **29**: 1711-1715.
12. van der Wal GE, Gouw AS, Kamps JA, *et al.* (2012) Angiogenesis in synchronous and metachronous colorectal liver metastases: the liver as a permissive soil. *Ann Surg*, **255**: 86.
13. Boroujeni MB, Boroujeni NB, Gholami M (2016) The effect of progesterone treatment after ovarian induction on endometrial VEGF gene expression and its receptors in mice at pre-implantation time. *Iran J Basic Med Sci*, **19**: 252-257.
14. Yakkundi A, Bennett R, Hernández-Negrete I, *et al.* (2015) FKBPL is a critical antiangiogenic regulator of developmental and pathological angiogenesis. *Arterioscl Throm Vas*, **35**: 845-54.
15. Leng R, Zha L, Tang L (2014) MiR-718 represses VEGF and inhibits ovarian cancer cell progression. *Febs Letters*, **588**: 2078-2086.
16. Yuan SJ, Qiao TK, Qiang JW, *et al.* (2017) The value of DCE-MRI in assessing histopathological and molecular biological features in induced rat epithelial ovarian carcinomas. *J Ovarian Res*, **10**: 65.
17. Shen W, Li H L, Liu L, *et al.* (2017) Expression levels of PTEN, HIF-1 $\alpha$ , and VEGF as prognostic factors in ovarian cancer. *Eur Rev Med Pharmacol*, **21**: 2596.
18. Macari M, Megibow AJ, Balthazar EJ (2007) A pattern approach to the abnormal small bowel: observations at MDCT and CT enterography. *Ajr Am J Roentgenol*, **188**: 1344-1355.
19. Pilleul F, Penigaud M, Milot L, *et al.* (2006) Possible small-bowel neoplasms: contrast-enhanced and water-enhanced multidetector CT enteroclysis. *Radiology*, **241**: 796.
20. Willmann JK, Lutz AM, Paulmurugan R, Patel MR, Chu P, Rosenberg J, Gambhir SS (2008) Dual-targeted contrast agent for US assessment of tumor angiogenesis *in-vivo*. *Radiology*, **248**: 936-44.
21. Hervey-Jumper SL, Garton HJ, Lau D, *et al.* (2014) Differences in vascular endothelial growth factor receptor expression and correlation with the degree of enhancement in medulloblastoma. *J Neurosurg Pediatr*, **14**: 121-128.
22. Ludwin I, Ludwin A, Wiechec M, *et al.* (2017) Accuracy of hysterosalpingo-foam sonography in comparison to hysterosalpingo-contrast sonography with air/saline and to laparoscopy with dye. *Hum Reprod*, **32**: 758-769.
23. Cosgrove D (2003) Angiogenesis imaging--ultrasound. *Brit J Radiol*, **76(1)**: S43-9.
24. Fokas E, Hänze J, Kamlah F, *et al.* (2010) Irradiation-dependent effects on tumor perfusion and endogenous and exogenous hypoxia markers in an A549 xenograft model. *Int J Radiat Oncol Biol Phys*, **77**: 1500-1508.
25. Wang JY, Lv FQ, Fei X, *et al.* (2011) Study on the characteristics of contrast-enhanced ultrasound and its utility in assessing the microvessel density in ovarian tumors or tumor-like lesions. *Int J Biol Sci*, **7**: 600-606.

